Passive and Active Electrical Balance Duplexers

Leo Laughlin, *Member, IEEE,* Chunqing Zhang, *Member, IEEE,* Mark A. Beach, *Member, IEEE,* Kevin A. Morris, *Member, IEEE,* and John L. Haine, *Member, IEEE*

***Abstract*—Electrical balance duplexing enables simultaneous transmit and receive from a single antenna, however the transmit-to-receive isolation depends on the ability of the balancing algorithm to determine the correct balancing impedance. A novel balancing algorithm based on in-situ characterization of the duplexer self-interference channel is proposed. The algorithm requires no a-priori knowledge of the antenna impedance or hybrid junction characteristics, and automatically compensates for circuit imperfections. A novel balancing network implementation which uses active signal injection is also proposed. A hardware prototype implementing the proposed balancing algorithm and combining passive and active balancing techniques has achieved 81.5dB isolation over an 80MHz bandwidth.**

***Keywords*—Duplexers, Full-duplex, Electrical Balance Duplexer, Self-interference cancellation, 5G enabling technologies.**

I. Introduction

FUTURE CELLULAR HANDSETS will be required to support numerous radio access technologies, using a variety of duplexing modes over a wide range of operating frequencies. Limitations in current Radio Frequency (RF) front-end technologies mean novel duplexing solutions are required to enable the multi-band multi-mode transceivers of the future. Electrical Balance Duplexers (EBDs) [1]–[5] can provide high transmit-to-receive (Tx-Rx) isolation whilst facilitating simultaneous transmission and reception from a single antenna. In Frequency Division Duplexing (FDD) applications, EBDs could reduce device cost and size as compared to the current technology, where multiple off-chip acoustic resonator filters are required [2]. In a Full-Duplex application [5]–[9] EBDs can be combined with further self-interference cancellation techniques to create a single antenna full-duplex transceiver architecture [5]. A drawback of EBDs is loss in the Tx and Rx paths, however this can be mitigated by employing a noise matched receiver design [1], [2]. EBDs can be implemented on-chip and are tunable over wide frequency ranges, making them well suited to multi-band operation in low cost small form factor devices.

The ideal EBD achieves high isolation when its *balancing impedance* equals the antenna impedance. The antenna impedance is time-variant due to environmental effects, and the balancing impedance must be dynamically adjusted to maintain isolation. Re-balancing the duplexer every 10ms is sufficient to maintain isolation [3]. The Tx-Rx isolation is determined by how accurately the balance impedance can assume the required value, and therefore obtaining high isolation requires correspondingly high accuracy in the tunable balancing impedance (an on-chip 15-bit digitally tunable complex impedance was reported in [1], acheiving >55dB of Tx-Rx isolation). The required tuning range of the balancing impedance depends on the range of variation in the antenna impedance, however antenna tuning can be applied to limit this variation [3].

Tracking processes can be effective at maintaining balance during operation [4], however in cellular transceivers, which seldom operate continuously, a fast and effective method of obtaining the correct balance setting whenever the modem enters active mode is essential. Balancing algorithms reported in the literature [4], [10], find this *initial balance* using iterative processes which require many self-interference channel measurements, and are thus unduly slow. To the authors' knowledge, no deterministic balancing algorithms have been reported, and there has been no published analysis of self-interference channels in non-ideal EBDs.

Active RF signal cancellation can be used to suppress self-interference and increase Tx-Rx isolation [7], [9], [11]. The level of cancellation is limited by noise and imperfections in the Tx chains [8], [9], however noise cancellation [12], [13], and linearization [14] can be used to increase performance.

In this brief we present an analysis of self-interference coupling in EBDs and from this we derive a novel deterministic balancing algorithm. Additionally, we present a novel active method for implementing the EBD balancing subsystem. Section II introduces the balancing algorithm and section III proposes the active balancing technique. Section IV presents results from a hardware prototype, and section V concludes.

II. EB Duplexer Balancing Algorithm

A. Ideal EB Duplexer

The S-matrix equation for an ideal EBD is given by

$$\begin{bmatrix} b_T \\ b_R \\ b_A \\ b_B \end{bmatrix} = \begin{bmatrix} 0 & 0 & k & l \\ 0 & 0 & l & -k \\ k & l & 0 & 0 \\ l & -k & 0 & 0 \end{bmatrix} \begin{bmatrix} a_T \\ a_R \\ a_A \\ a_B \end{bmatrix} \quad (1)$$

where k is the coupling coefficient, and $l = \sqrt{1-k^2}$ (since the ideal hybrid is lossless), a_T, a_R, a_A, a_B are the incident signals at the transmit, receive, antenna, and balance ports respectively, and b_T, b_R, b_A, b_B are the corresponding scattered signals [2]. Assuming matched impedances at the transmit and receive ports, and reflection coefficients of $\Gamma_A(\omega)$ and $\Gamma_B(\omega)$ at the antenna and balance ports respectively (relative to the

Manuscript received March 31, 2015; revised August 7, 2015; accepted August 12, 2015. Date of publication: December 2015. This research is supported by the UK EPSRC through the CDT in Communications (EP/I028153/1), and through iCASE sponsorship by u-blox AG.

L. Laughlin, C. Zhang, M. A. Beach, and K. A. Morris are with the Department of Electrical and Electronic Engineering, University of Bristol, BS8 1UB, UK. e-mail: Leo.Laughlin@bristol.ac.uk.

J. L. Haine is with u-blox AG, 8800 Thalwil, Switzerland.

Digital Object Identifier

matched impedance), simple S-matrix manipulation yields an expression for the Tx-Rx transfer function as

$$G(\omega) = \frac{b_R(\omega)}{a_T(\omega)} = kl\left(\Gamma_A(\omega) - \Gamma_B(\omega)\right) \tag{2}$$

and thus for the ideal duplexer, the self-interference channel is a linear function of $\Gamma_B(\omega)$. The balancing algorithm presented herein is based on multiple measurements of G, taken whilst Γ_B is set to different known values, to obtain a system of simultaneous equations. For example, we may rewrite (2) in a more general form by substituting $P(\omega) = kl\Gamma_A(\omega)$ and $Q(\omega) = -kl$ such that

$$G(\omega) = P(\omega) + Q(\omega)\Gamma_B(\omega) \tag{3}$$

and making two measurements of G for two values of Γ_B, and yields

$$G_1(\omega) = P(\omega) + Q(\omega)\Gamma_{B_1}(\omega) \tag{4}$$
$$G_2(\omega) = P(\omega) + Q(\omega)\Gamma_{B_2}(\omega). \tag{5}$$

This can be solved to determine P and Q, such that

$$Q(\omega) = \frac{G_2(\omega) - G_1(\omega)}{\Gamma_{B_2}(\omega) - \Gamma_{B_1}(\omega)} \tag{6}$$
$$P(\omega) = G_1(\omega) - Q(\omega)\Gamma_{B_1}(\omega). \tag{7}$$

Thus we have fully characterized the Tx-Rx gain as a function of the balancing reflection coefficient. *The reflection coefficient value required to balance the duplexer is then simply the root of* (3). No knowledge of k, l, or $\Gamma_A(\omega)$ is required to balance the duplexer in this way, and thus this method represents a characterization process which determines the correct balancing impedance in a system with an unknown antenna impedance and unknown hybrid junction characteristics. The method therefore automatically compensates for manufacturing variations in the hybrid. Measurement of $G(\omega)$ requires no additional hardware as this can be readily performed using the transmitter and receiver. Compared to existing techniques [4], [10], the number of measurements required is far fewer, thus reducing the initial balancing time. Furthermore, this algorithm does not require absolute knowledge of the balancing impedance. For example, it can be shown that substituting $\Gamma_B(\omega) = X(\omega)\Gamma'_B(\omega)+Y(\omega)$ into (3) to model inaccuracy in the control of the balancing reflection coefficient yields an expression of the same form as (3). Thus, control of the *absolute value* of the balancing impedance is not necessary in order to balance the duplexer: knowing the *difference* between values is sufficient. Similarly, it can be shown that the Tx-Rx gain measurements are only required to be differential rather than absolute, and therefore amplitude and phase error introduced by the transmit and receive chains will not affect the performance of this method provided the error is the same for each of the measurements. Since the measurement process can be performed extremely quickly ($\sim$100μs) [10] time varying circuit characteristics (e.g. the antenna impedance) will not affect the performance, as the variation is insignificant over the measurement process duration [3], [10].

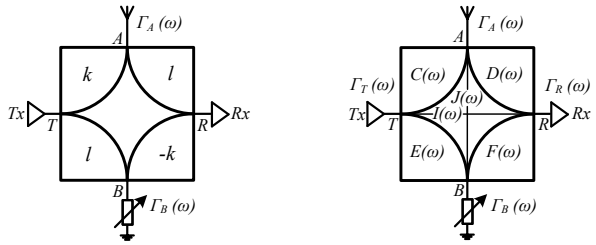

(a) Idealized EBD model (b) Realistic EBD model

Fig. 1. Two models of signal coupling and reflection in electrical balance duplexers.

B. Non-ideal EBD

The ideal EBD model (Fig. 1(a)) implicitly assumes that the hybrid junction is lossless, frequency invariant, and has zero direct coupling between opposite ports. Furthermore, although the ideal hybrid junction may not be symmetrical (i.e. k^2 is not necessarily 0.5), it has symmetry about the bottom left to top right diagonal of the S-matrix (*persymmetry*), which, for example, implies that the coupling between the transmit port and antenna port is identical to the coupling between the balance port and the receive port. In a practical hybrid, these assumptions may not be valid. The hybrid junction component of the EBD may typically be implemented using a hybrid transformer, which will suffer from imperfections including loss, direct coupling between opposite ports, frequency selective coupling, and the persymmetry of the S-matrix may only be approximate (Fig. 1(b)). Modifying (1) to take all of these imperfections into account gives

$$\begin{bmatrix} b_T(\omega) \\ b_R(\omega) \\ b_A(\omega) \\ b_B(\omega) \end{bmatrix} = \begin{bmatrix} W(\omega) & I(\omega) & C(\omega) & E(\omega) \\ I(\omega) & X(\omega) & D(\omega) & F(\omega) \\ C(\omega) & D(\omega) & Y(\omega) & J(\omega) \\ E(\omega) & F(\omega) & J(\omega) & Z(\omega) \end{bmatrix} \begin{bmatrix} a_T(\omega) \\ a_R(\omega) \\ a_A(\omega) \\ a_B(\omega) \end{bmatrix}. \tag{8}$$

For mathematical brevity henceforth this analysis applies to a frequency invariant system in order to that we may dispense with "(ω)" in the notation, however this analysis also holds for the frequency selective case. Also for mathematical brevity the following example assumes matched impedances at the transmit and receive ports and zero values for W, X, Y, and Z. Under these assumptions, S-matrix manipulation of (8) gives the Tx-Rx transfer function as

$$G = I + \frac{C\Gamma_A D}{1-\Gamma_A\Gamma_B J^2} + \frac{E\Gamma_B F}{1-\Gamma_A\Gamma_B J^2} + \frac{C\Gamma_A J\Gamma_B F}{1-\Gamma_A\Gamma_B J^2} + \frac{E\Gamma_B J\Gamma_A D}{1-\Gamma_A\Gamma_B J^2}. \tag{9}$$

Observing (9), we may note that this is not of the form of (3), and therefore it appears that the non-ideal duplexer modeled using (8) cannot be balanced by the proposed algorithm as described thus far. However, the following analysis will show that (9) can be approximated by a polynomial of Γ_B, allowing the proposed method to be applied.

The last four terms of (9) can each be re-written as the sum of an infinite geometric series with ratio $\Gamma_A\Gamma_B J^2$ (which

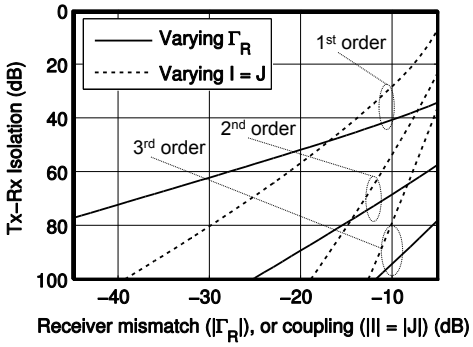

Fig. 2. Simulated effect of receiver mismatch or direct coupling on balancing algorithm performance in a noiseless system.

results in the $1 - \Gamma_A \Gamma_B J^2$ denominator of these terms). This is a consequence of reverberating signals within the hybrid junction, as the direct coupling path J makes it possible for signal components to be reflected back and forth between the antenna and balance port multiple times, and thus, in theory, there are an infinite number of paths between the transmitter and receiver. For example, for $(\Gamma_A \Gamma_B J^2) < 1$, we may re-write the last term of (9) as

$$\begin{aligned} \frac{E\Gamma_B J \Gamma_A D}{1 - \Gamma_A \Gamma_B J^2} &= E\Gamma_B J \Gamma_A D \sum_{n=0}^{\infty} (\Gamma_A \Gamma_B J^2)^n \\ &= DE\Gamma_A J \Gamma_B + DE{\Gamma_A}^2 J^3 {\Gamma_B}^2 \\ &\quad + DE{\Gamma_A}^3 J^5 {\Gamma_B}^3 + DE{\Gamma_A}^4 J^7 {\Gamma_B}^4 + \ \ldots \ . \end{aligned} \tag{10}$$

By expanding the other terms of (9) in this manner, and grouping coefficients of ${\Gamma_B}^n$, it can be shown that (9) can be expressed as a polynomial of Γ_B, with coefficients L_n, such that

$$G = \sum_{n=0}^{\infty} L_n {\Gamma_B}^n. \tag{11}$$

Although for brevity this example has not considered all imperfections, it is left to the reader to consider that modeling all circuit imperfections (i.e. mismatch at all duplexer ports and non-zero values in all elements of the S-matrix) will result in an expression that can be written as a polynomial of Γ_B. This can be explained by considering that self-interference arriving at the receiver port can be divided into components which have not been reflected at the balance port, components which have been reflected at the balance port once, components reflected at the balance port twice, and so on.

The circuit imperfections mean that the self-interference channel is no longer a linear function of Γ_B (as was the case in (3)). Therefore, the method presented in II-A cannot be used to fully characterize the channel. However, (3) is a linear approximation of (11), where the infinite summation has been truncated to the first two terms. A more accurate approximation of G in the non-ideal case would be a quadratic function (i.e. the first three terms of (11)), and a more accurate model still would be a cubic function. The proposed algorithm can be extended to estimate these higher order terms. For example, taking three measurements of G for three different values of Γ_B allows the first three terms of (11) to be estimated, and from this a 2nd order approximation of (11) can be formed. Similarly, four measurements can yield a 3rd order approximation. Solving these higher order systems will result in more than one root, however throughout this investigation it was observed that only one of these will satisfy $|\Gamma_B| < 1$, (i.e. a passive network). Higher order balancing algorithms may therefore increase accuracy in non-ideal EBDs. Table I gives the number of measurements and complex operations required to balance the duplexer at a single frequency point. Although the higher order algorithms increase the number of operations, this still remains comparatively low and requires far fewer measurements than iterative methods [4], [10].

TABLE I. NUMBER OF OPERATIONS IN BALANCING ALGORITHM.

Algorithm	Measurements	+/-	×	÷	$\sqrt{\cdot}$	$\sqrt[3]{\cdot}$	$\lvert . \rvert$	< 1
1st order	2	4	1	2	0	0	0	0
2nd order	3	29	28	7	1	0	1	1
3rd order	4	127	154	18	1	1	2	2

TABLE II. SIMUALTED TX-RX ISOLATION AT THE BALANCING FREQUENCY FOR DIFFERENT MEASUREMENT SIGNAL-TO-NOISE RATIOS.

	SNR					
Algorithm	noiseless	50dB	40dB	30dB	20dB	10dB
1st order	69.2dB	55.1dB	45.4dB	35.5dB	25.7dB	17.2dB
2nd order	131.8dB	59.4dB	49.3dB	39.3dB	28.6dB	19.1dB
3rd order	194.4dB	64.0dB	54.0dB	43.0dB	33.9dB	23.8dB

C. Simulated performance

Simulation was used to investigate the performance of the 1st, 2nd, and 3rd order balancing algorithms in two different non-ideal EBDs: one with direct coupling between ports (non-zero I and J), and one with receiver mismatch. The simulation assumes an antenna return loss of 6dB (a worst case for cellular handsets), and a symmetrical hybrid junction with 0.5dB insertion loss at each port. Assuming noiseless measurement of $G_1 ... G_4$, the simulation determines the Tx-Rx isolation achieved at the balancing frequency point, as either the receiver port reflection coefficient (Γ_R), or the direct opposite port coupling channels (I and J) are varied, thereby allowing the performance of the three algorithms to be compared when subject to these two specific imperfections. In the latter case I and J are assumed to be equal. Results are presented in Fig. 2. These demonstrate that circuit imperfections have a significant detrimental impact on the performance of the algorithm, however, including higher order terms in the self-interference channel model is an effective way of mitigating this. The results also demonstrate that for circuit imperfections which would be typical of a real system, (for example opposite port coupling of -20dB or receiver mismatch of -15dB), higher order balancing algorithms would be necessary to obtain adequate balancing accuracy. The simulation was also used to investigate the impact of measurement noise on the performance of the algorithm. In the simulated duplexer as described above, with Γ_R = 0 and I = J = -25dB, the resulting isolation was observed as the SNR of the channel measurements, $G_1 ... G_4$,

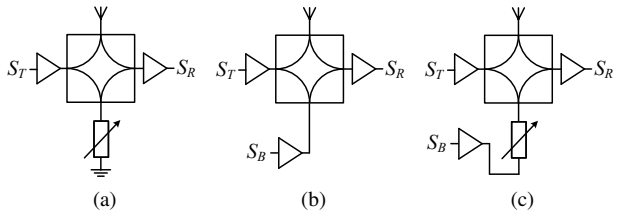

Fig. 3. (a) Passive EBD. (b) Active EBD. (c) Compound EBD.

was varied. Results are given in Table II, showing that high SNR is required to acheive high isolation. This is a drawback of the proposed method, as achieving high SNR measurements may increase the cost and/or computational expense. However, a less accurate initial balance estimate would still remain useful, for example as the starting point for a further iterative balancing process, thereby reducing convergence time.

III. Active Balancing

In passive EBDs (Fig. 3(a)), a simple balancing network (such as a single pole RC circuit [1], [2], [5]) results in poor isolation at wider bandwidths, as the bandwidth over which the balancing impedance can mimic the antenna impedance is limited [5]. Implementing a tunable passive balancing network which can provide the correct impedance trajectory across wide bandwidths would significantly increase the size and cost of the balancing subsystem. Instead, it is proposed that an auxiliary transmitter can be used to inject a *balancing signal* which is equal to the signal which would have been reflected by such a balancing network (Fig. 3(b)). The proposed method generates the balancing signal in digital baseband, where high order filtering can be applied to generate a balancing signal which is accurate over wide bandwidths. The complexity required to achieve wideband isolation is thereby moved from passive components to baseband DSP, reducing cost, however performance is limited by Tx noise and imperfections, and this could potentially increase the receiver noise floor [8], [9].

To determine the balancing signal, we may consider the balancing signal injection as a *cancellation process* [11]. For example, we may model the signal arriving at the receiver, S_R as

$$S_R(\omega) = G(\omega)S_T(\omega) + B(\omega)S_B(\omega) \tag{12}$$

where, as before, $G(\omega)$ is the self-interference channel, and $B(\omega)$ is the channel between the balance port and receiver port (the *balancing channel*), and $S_T(\omega)$ and $S_B(\omega)$ are the transmit and balancing signals respectively. $G(\omega)$ and $B(\omega)$ can be measured by transmitting known signals from each transmitter whilst the other transmitter is inactive, and measuring the signals which result at the receiver. The balancing signal can then be calculated as [11]

$$S_B(\omega) = -\frac{G(\omega)S_T(\omega)}{B(\omega)}. \tag{13}$$

Fig. 3(c) depicts the proposed *compound EBD* combining both passive and active balancing techniques. The passive tunable impedance component is adjusted to provide passive isolation, and a balancing signal is also injected to provide additional active self-interference cancellation. Due to the much higher level of passive isolation obtained by tuning the impedance at the balance port, the cancellation process in the compound EBD occurs at a much lower power level as compared to the active EBD, increasing the overall isolation. The compound EBD will therefore also have less of an impact on the receiver noise floor compared to the active EBD.

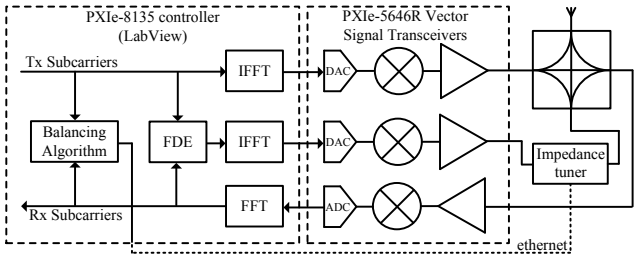

Fig. 4. Hardware prototype compound EBD.

IV. Hardware Prototype

A hardware prototype compound EBD was constructed. A Focus Microwaves model 1808 electromechanical impedance tuner was used in the passive balancing subsystem, transforming the 50Ω auxiliary transmitter output impedance in order to present the correct passive impedance at the balance port (as determined by the balancing algorithm). The transmitters and receiver were implemented using National Instruments PXIe-5646R Vector Signal Transceivers, controlled by a PXIe-8135 controller. The balancing algorithm and balancing signal generation are both implemented in LabView and run on the controller, which is connected to the impedance tuner via ethernet. To enable frequency selective operation in the balancing signal generation, the prototype employs an LTE-like OFDM physical layer, with a subcarrier spacing of 15kHz, and an 80MHz bandwidth. The passive balancing process runs first, using the balancing algorithm and controlling the impedance tuner to maximize passive isolation at the balancing frequency (1.9GHz). Once passive balancing is complete, the system measures $G(\omega)$ and $B(\omega)$ at each subcarrier frequency and performs Frequency Domain Equalization on the transmit signal to generate the balancing signal. To demonstrate the effect of non-ideal hybrid characteristics, measurements were taken for two different hybrid junctions: a Krytar model 1831 hybrid coupler, with measured opposite port coupling of <-35dB, and Sage Wireline hybrid [15], with measured opposite port coupling of -18dB.

To investigate the effect of circuit imperfections on the performance of the balancing algorithm, the passive EBD isolation at the balancing frequency was measured for a range of different known impedances at the antenna and receiver ports, using both the Krytar and Sage hybrids. Results are given in Table III. The measurements demonstrate that, even in the Krytar hybrid, the performance of the first and second order algorithms worsens as antenna mismatch and receiver mismatch become larger, however the higher order balancing algorithms are effective at compensating for the circuit imperfections. In most cases, the Sage hybrid results in worse performance as compared to the corresponding measurement performed on the Krytar hybrid, demonstrating the detrimental

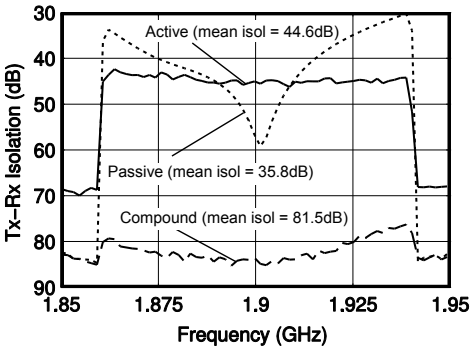

Fig. 5. Measured Tx-Rx isolation for the passively balanced EBD, the actively balanced EBD, and the compound EBD.

effect of opposite port coupling on the performance of the algorithm. In all measurements, the 3rd order balancing algorithm achieved approximately 62dB of isolation, this being comparable to existing techniques [4], [10] and limited by the accuracy of the impedance tuner.

Measurements were taken when using passive balancing only, when using active balancing only, and when using compound balancing. Fig. 5 compares the measured Tx-Rx isolation frequency response for the three EBD balancing methods using the Sage hybrid and a Taoglas PAD710 multi-band cellular antenna (Γ_A = -11dB). Without any adaptive balancing (i.e. with a 50Ω impedance at the balance port), the EBD achieves only 18dB of Tx-Rx isolation. The passive only method achieves 58dB of isolation at the balancing frequency but as little as 30dB at the band edges, whereas the active method provides the approximately the same level of isolation (44.6dB) across the entire system bandwidth, this being limited by the EVM of the transmit chains. The compound EBD achieves significantly higher isolation of 81.5dB. The noise floor of the prototype system was increased by approximately 15dB when using active EBD as compared to the passive EBD, however, the compound EBD showed no additional noise compared to the passive EBD.

V. Conclusion

A novel EBD balancing algorithm has been proposed and implemented. The algorithm requires fewer measurements and arithmetic operations than existing techniques [4], [10], but is limited by measurement SNR. Simulations and measurements demonstrate that approximating the self-interference channel using higher order polynomials can successfully compensate for EBD circuit imperfections.

Balancing the EBD using active signal injection has also been proposed and implemented. The active balancing technique does not rely on tunable passive components, and can balance the duplexer over wide bandwidths. A prototype based on instrumentation grade hardware has combined the passive and active methods to achieve 81.5dB of isolation over 80MHz. Further work is required to assess the impact of practical hardware imperfections on the performance of the techniques presented herein.

TABLE III. Measured Tx-Rx isolation at the balancing frequency when using 1ST, 2ND, and 3RD order algorithms in various passive EBDs with different circuit imperfections.

Hybrid	Γ_A	Γ_R	1st order	2nd order	3rd order,
Krytar	match	match	63.2dB	62.8dB	62.1dB
Krytar	-12dB	match	54.5dB	57.2dB	61.2dB
Krytar	-6dB	match	52.7dB	55.2dB	60.2dB
Krytar	-6dB	-20dB	40.1dB	56.4dB	63.6dB
Krytar	-6dB	-10dB	30.3dB	47.7dB	62.9dB
Sage	match	match	46.7dB	60.5dB	66.4dB
Sage	-12dB	match	42.6dB	54.2dB	60.0dB
Sage	-6dB	match	39.0dB	49.0dB	62.9dB
Sage	-6dB	-20dB	38.7dB	51.9dB	63.9dB
Sage	-6dB	-10dB	34.2dB	44.3dB	58.0dB

Acknowledgment

The authors thank Mici McCullagh of u-blox for insightful discussions and Taoglas for providing the antenna.

References

[1] M. Mikhemar, *et al.*, "A Multiband RF Antenna Duplexer on CMOS: Design and Performance," *Solid-State Circuits, IEEE J.*, vol. 48, no. 9, pp. 2067–2077, 2013.

[2] S. H. Abdelhalem, *et al.*, "Hybrid Transformer-Based Tunable Differential Duplexer in a 90-nm CMOS Process," *Microw. Theory Tech. IEEE Trans.*, vol. 61, no. 3, pp. 1316–1326, 2013.

[3] L. Laughlin, *et al.*, "Electrical balance duplexing for small form factor realization of in-band full duplex," *IEEE Commun. Mag.*, vol. 53, no. 5, pp. 102–110, May 2015.

[4] S. H. Abdelhalem, *et al.*, "Tunable CMOS Integrated Duplexer With Antenna Impedance Tracking and High Isolation in the Transmit and Receive Bands," *IEEE Trans. Microw. Theory Tech.*, vol. 62, no. 9, pp. 2092–2104, Sept. 2014.

[5] L. Laughlin, *et al.*, "Optimum Single Antenna Full Duplex Using Hybrid Junctions," *IEEE J. Sel. Areas Commun.*, vol. 32, no. 9, pp. 1653–1661, Sept. 2014.

[6] S. Chen, *et al.*, "Division-free duplex for wireless applications," *Electron. Lett.*, vol. 34, no. 2, pp. 147–148, 1998.

[7] A. Sabharwal, *et al.*, "In-Band Full-Duplex Wireless: Challenges and Opportunities," *IEEE J. Sel. Areas Commun.*, vol. 32, no. 9, pp. 1637–1652, Sept. 2014.

[8] A. Sahai, *et al.*, "On the Impact of Phase Noise on Active Cancelation in Wireless Full-Duplex," *IEEE Trans. Veh. Technol.*, vol. 62, no. 9, pp. 4494–4510, Nov. 2013.

[9] B. Debaillie, *et al.*, "Analog/RF Solutions Enabling Compact Full-Duplex Radios," *IEEE J. Sel. Areas Commun.*, vol. 32, no. 9, pp. 1662–1673, Sept. 2014.

[10] M. Mikhael, *et al.*, "A Full-Duplex Transceiver Prototype with In-System Automated Tuning of the RF Self-Interference Cancellation," in *Proc. 1st Int. Conf. 5G Ubiquitous Connect.* ICST, 2014, pp. 110–115.

[11] W. Schacherbauer, *et al.*, "An Interference Cancellation Technique for the Use in Multiband Software Radio Frontend Design," in *Microw. Conf. 2000. 30th Eur.*, 2000, pp. 1–4.

[12] M. Omer, *et al.*, "A PA-noise cancellation technique for next generation highly integrated RF front-ends," in *2012 IEEE Radio Freq. Integr. Circuits Symp.* IEEE, June 2012, pp. 471–474.

[13] J. Zhou, *et al.*, "Low-Noise Active Cancellation of Transmitter Leakage and Transmitter Noise in Broadband Wireless Receivers for FDD/Co-Existence," *IEEE J. Solid-State Circuits*, vol. 49, no. 12, pp. 3046–3062, Dec. 2014.

[14] R. Askar, *et al.*, "Active self-interference cancellation mechanism for full-duplex wireless transceivers," in *9th Int. Conf. Cogn. Radio Oriented Wirel. Networks Commun.*, 2014, pp. 539–544.

[15] API Technologies Corp., "Wireline and Wirepac Design Guide." [Online]. Available: http://micro.apitech.com/pdf/wireline/designguide.pdf Accessed: 2015-03-25.